BULLETIN OF THE EARTHQUAKE
RESEARCH INSTITUTE
UNIVERSITY OF TOKYO
Vol. 62 (1987) pp. 391-415

Report on DELP 1985 Cruises in the Japan Sea Part IV: Geomagnetic Anomalies over the Seamounts in the Yamato Basin

Keizo SAYANAGI[1], Nobuhiro ISEZAKI and Yasuo KITAHARA[2]

Department of Earth Sciences, Kobe University

(Received October 23, 1987)

Abstract

Seamount magnetic anomaly studies have been conducted on four seamounts (Yamato, B, Meiyo, Meiyo Daisan) in the Yamato Basin. These seamounts lie in the Yamato Seamount Chain trending approximately NE-SW parallel to the axis of the Basin. The total intensities and the three components of the geomagnetic field over four seamounts were measured. Bathymetric depths were measured by 12 kHz PDR. The minimum and maximum values of peak amplitudes of the magnetic anomalies observed over the Meiyo Seamount and B Seamount were 172 to 611 nT respectively. We have attemped to apply the method of Talwani to explain magnetic anomaly patterns over the four seamounts. The results indicate that B Seamount has normal magnetization and the remaining three seamounts have polarity reversals among different sections of each seamount. For all seamounts the declinations of magnetization lie around 0° or 180°. Thus, it appears that the Yamato Seamount Chain includes several polarity reversals and all seamounts have never been rotated relative to the average magnetic coordinate since their generation.

1. Introduction

The Japan Sea is one of the several marginal seas rimming the western Pacific (Fig. IV-1). It is separated by the Korea Plateau and Oki Bank-Yamato Ridge into the Japan Basin, the Yamato Basin, and the Tsushima Basin (Fig. IV-1). These basins are underlain by oceanic or sub-oceanic crusts (*e.g.*, LUDWIG *et al.*, 1975).

It has been believed that the Japan Sea was formed by crustal extension and seafloor spreading. Many models have been proposed to explain its origin and evolution (*e.g.*, ISEZAKI, 1973; GNIBIDENKO, 1979;

Present address: [1] Ocean Research Institute, University of Tokyo, Tokyo 164, Japan.
[2] Komatsu Co. Ltd., Kanagawa 254, Japan.

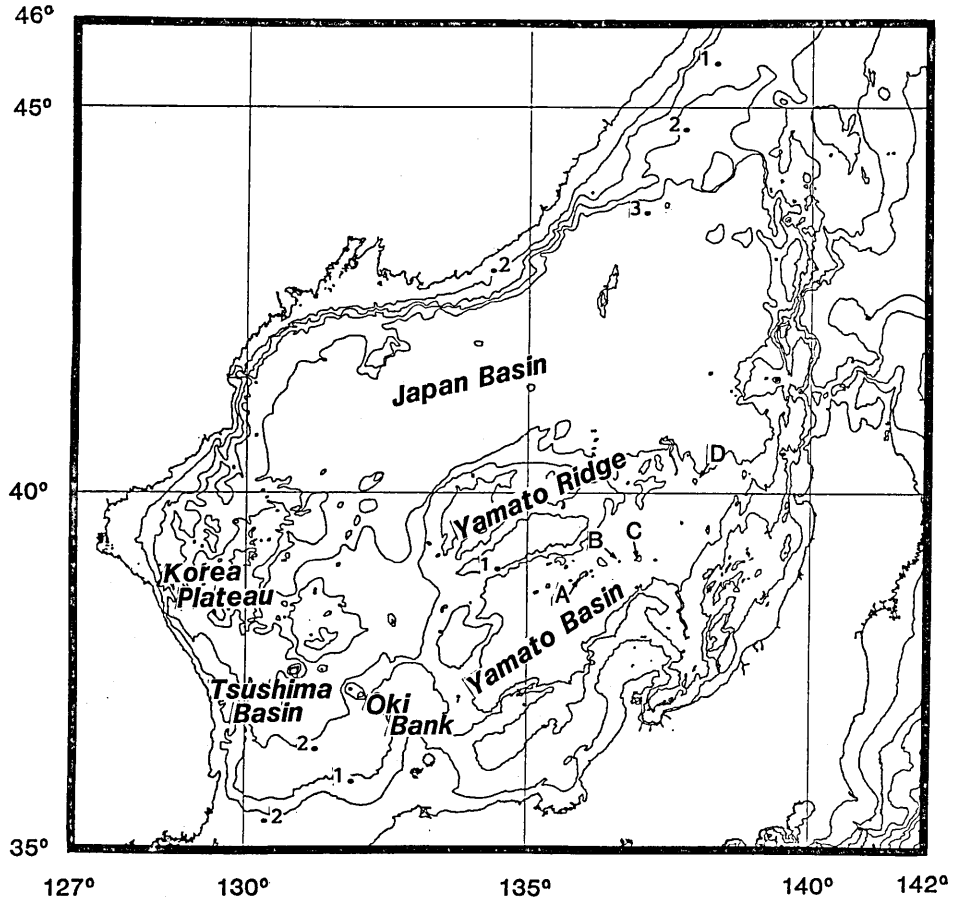

Fig. IV-1. Major physiographic features of the Japan Sea. A: Yamato Seamount, B: B Seamount, C: Meiyo Seamount and D: Meiyo Daisan Seamount.

OTOFUJI *et al.*, 1985a; b; TAMAKI, 1985; LALLEMAND and JOLIVET, 1986). The age and process of opening of the Japan Sea, however, remain somewhat controversial.

The following major methods have been used to determine the ages and processes of development of the ocean floors; (1) the determination of crustal and lithospheric thickness, (2) the age determination of bottom sediment or absolute dating of basement rocks obtained from deep sea drilling, and (3) the identification of magnetic anomaly lineations. Unfortunately, these three methods have not been successful yet for the Japan Sea. DSDP drillings could not make full penetration of the entire sedimentary sections in the Yamato and Japan Basins. The complicated magnetic anomaly pattern in the Japan Sea is not easily identified.

Numerous seamounts are spotted in the basins of the Japan Sea. The

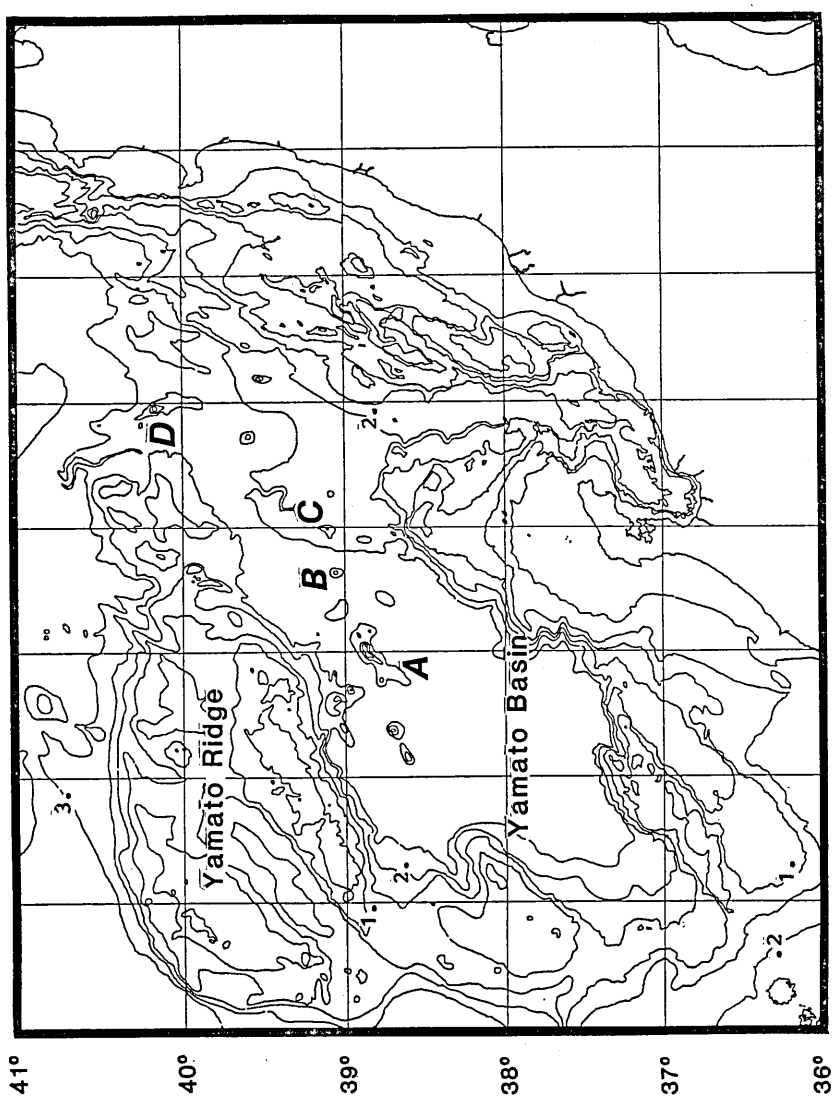

Fig. IV-2. Locations of four seamounts in the Yamato Basin. A: Yamato Seamount, B: B Seamount, C: Meiyo Seamount and D: Meiyo Daisan Seamount.

study of seamount magnetic anomalies gives us independent information of the previous methods with respect to seafloor spreading and tectonics of the Japan Sea.

During the summer of 1985 the DELP-85 WAKASHIO Cruise was undertaken for the purpose of collecting geologic samples and geophysical data in an attempt to understand the origin and tectonic history of the Japan Sea. The geomagnetic surveys of four seamounts (Yamato, B, Meiyo, and Meiyo Daisan) in the Yamato Basin were performed during the cruise.

The Yamato Seamount Chain, including the four seamounts studied in this paper, trend roughly NE-SW (Fig. IV-2). It is proposed that the Yamato Seamount Chain can be divided into two lines of topographic highs, the Yamato Seamount Chain in narrow sense and the Yamato Basin Ridge, in part VII of this report (KIMURA *et al.*, 1987). The direction is almost parallel to the axis of the Yamato Basin. This prominent topographic feature suggests that the seamount chain is related to the generation of the Yamato Basin. The purpose of this study is to clarify the evolution of the Yamato Seamount Chain from the magnetization of four seamounts. The information obtained from seamount studies will give us some interesting insights to the origin and development of the Japan Sea.

2. Method of Measurement

The block diagram of the system used in this survey is shown in Fig. IV-3. The system is called the STCM (Shipboard Three Component Magnetometer) system, which was developed by Isezaki and others since 1977 (*e.g.*, ISEZAKI *et al.*, 1981). For geomagnetic investigation we measured the following items using this system;

(1) total intensity of the geomagnetic field by a proton precession magnetometer (0.1 nT),

(2) three components of the geomagnetic field by STCM (25 nT),

(3) bathymetric depth by echo sounding techniques with a 12 kHz source (one meter),

(4) ship's position by means of Loran-C receiver (50 m),

(5) ship's heading by a gyrocompass (1′),

(6) ship's rolling and pitching angles by a vertical gyroscope (10′).

The measurement accuracy of each instrument is presented in the parentheses. All data signals are transferred to a microcomputer through input/output interface boards and then recorded on a floppy disk every one minute. They are also printed out at the same time. More details of this system has been reported by ISEZAKI (1986).

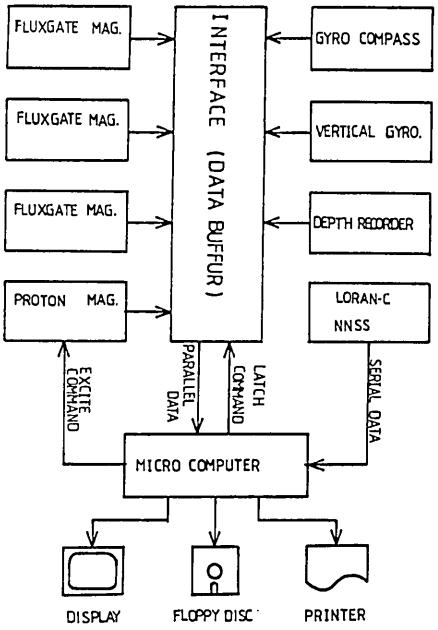

Fig. IV-3. Block diagram of the STCM system. (ISEZAKI, 1986).

3. Description of the Data

3.1. Yamato Seamount

1) Bathymetry:

The bathymetric contour map of Yamato Seamount is shown in Fig. IV-4. The seamount is the largest in volume in the Yamato Seamount Chain, including four peaks as denoted by A1, A2, A3, and A4 (Fig. IV-4). The volcano is elongated in a NE-SW direction. The shallowest peak is A2, which rises about 1790 m from the basin floor to a depth of 812 m.

2) Magnetic Anomalies:

Fig. IV-5 shows the total intensity anomalies. The anomalies have three positive and five negative peaks, though they are complicated with short wavelength anomalies. The largest value (503 nT) of peak to peak amplitudes is found over the bathymetric peak A2.

3.2. B Seamount

1) Bathymetry:

B Seamount, whose summit (B1) lies at a depth of 1847 m, is 753 m in height (Fig. IV-8). It is conelike with spurs protruding from the south and west flanks. The dimension is the smallest of all four seamounts.

2) Magnetic Anomalies:

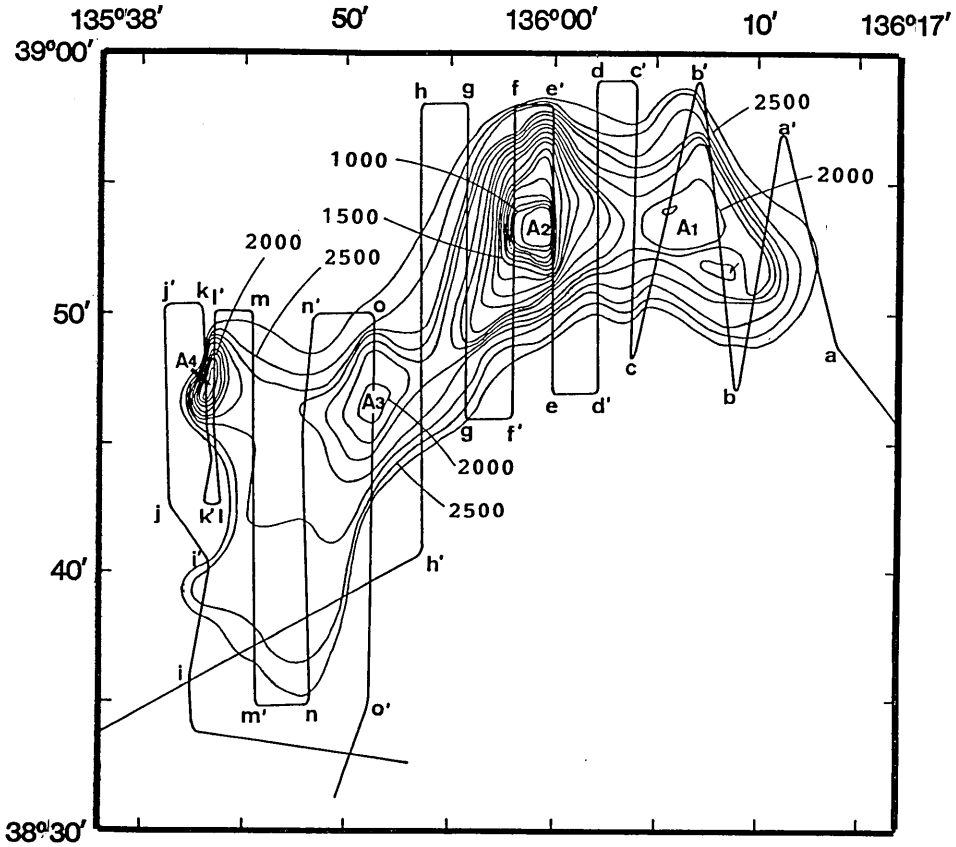

Fig. IV-4. Bathymetric contours of Yamato Seamount. Lines a to o′ are ship tracks. A1, A2, A3 and A4 denote four peaks of this seamount. Contour interval is 100 m.

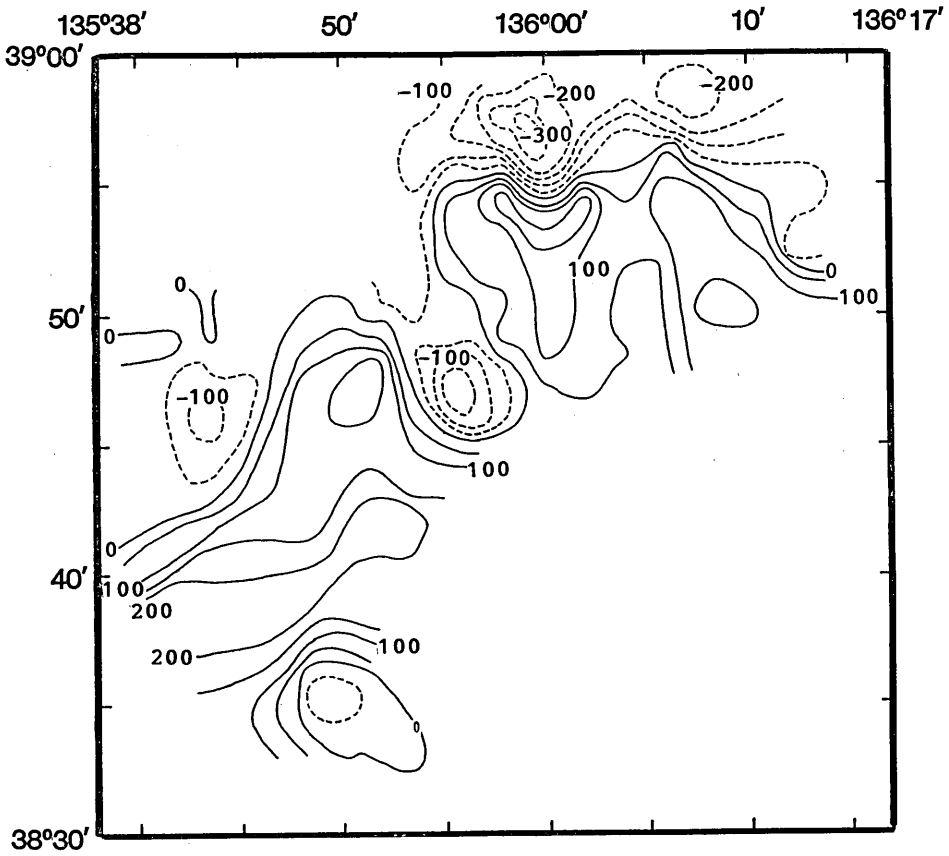

Fig. IV-5. Total intensity anomaly contours of Yamato Seamount. Contour interval is 50 nT.

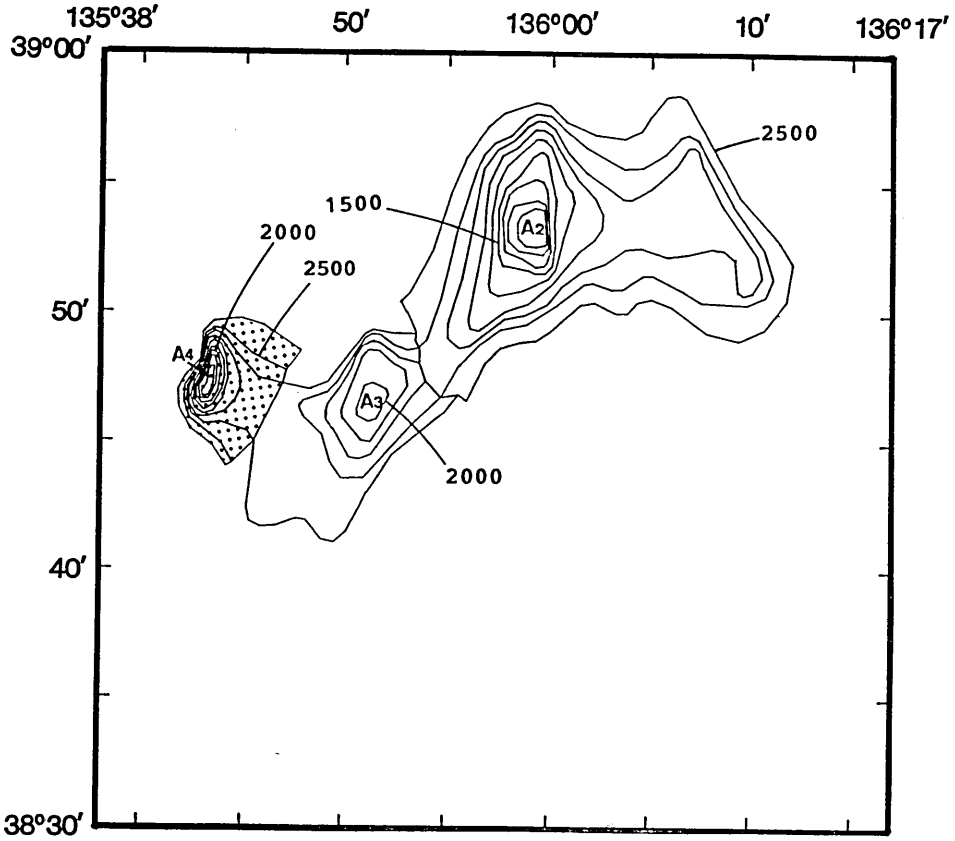

Fig. IV-6. Bathymetric model of Yamato Seamount. The white sections are normally magnetized. The dotted section is reversely magnetized. Contour intervals are 200 m for A2 and 100 m for A3 and A4.

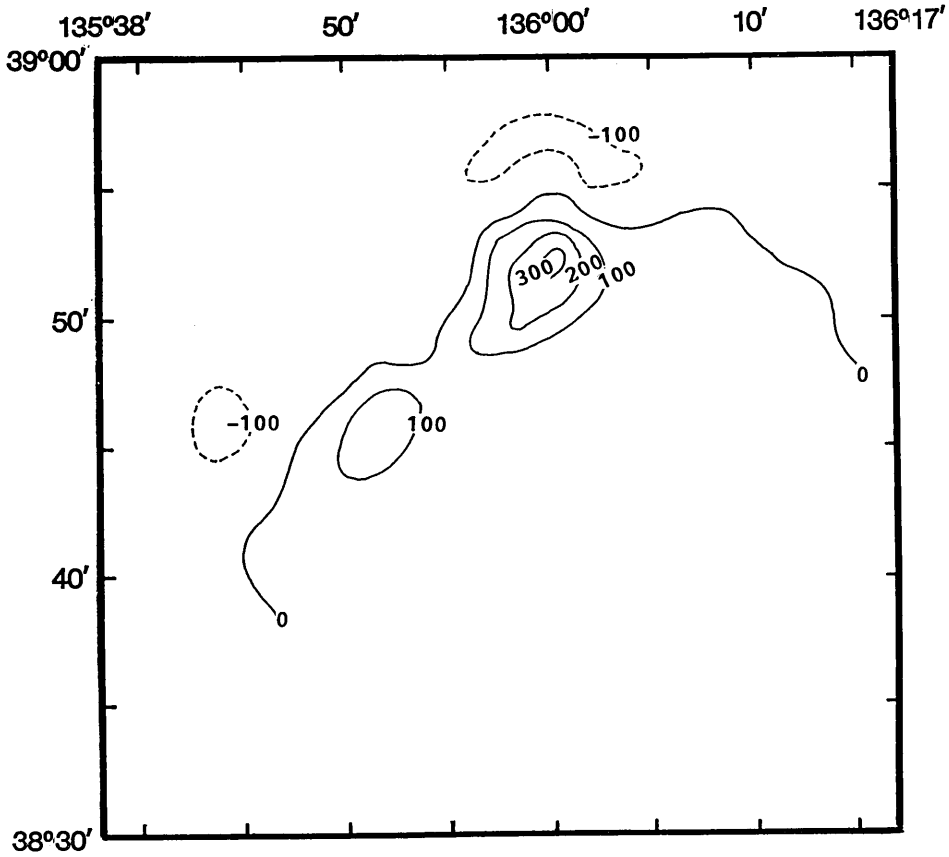

Fig. IV-7. Calculated anomaly contours of Yamato Seamount. Contour intervals is 100 nT.

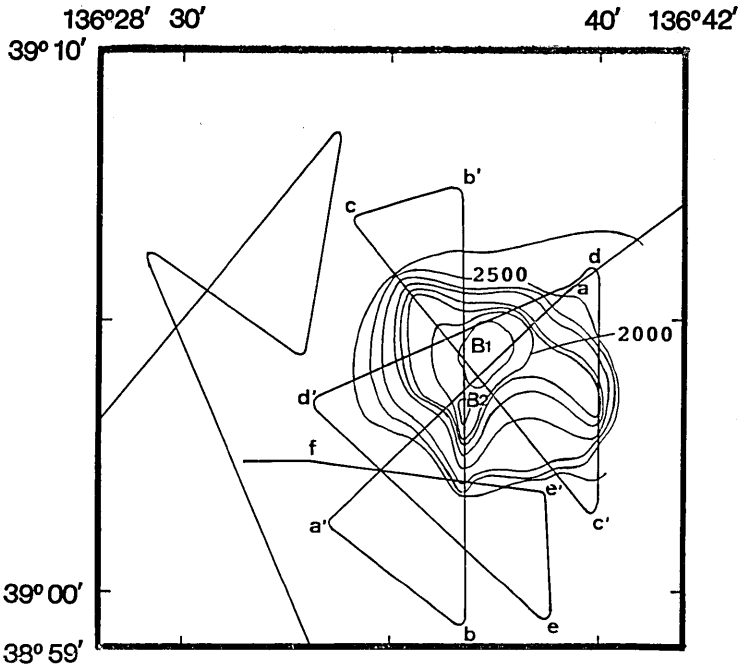

Fig. IV-8. Bathymetric contours of B Seamount. Lines a to f are ship tracks. B1 and B2 denote two bathymetric peaks. Contour interval is 100 m.

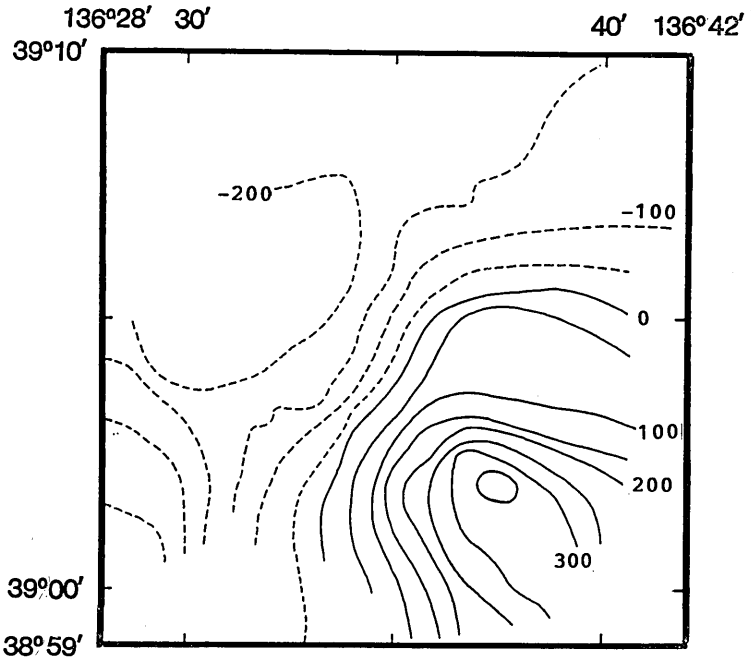

Fig. IV-9. Total intensity anomaly contours of B Seamount. Contour interval is 50 nT.

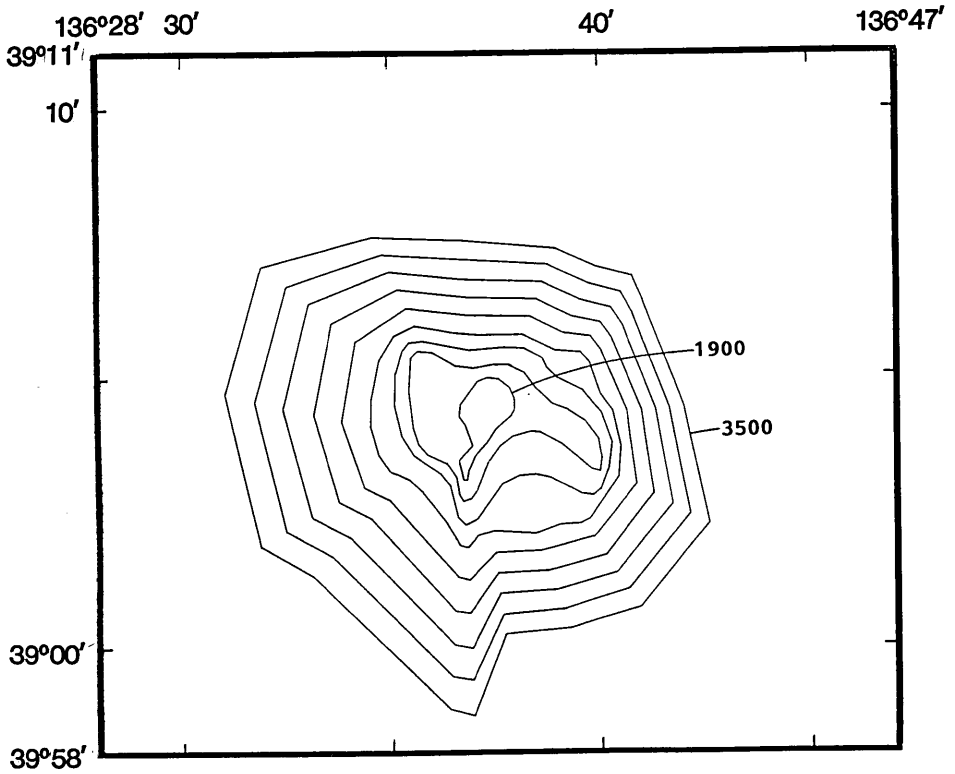

Fig. IV-10. Bathymetric model of B Seamount. Contour interval is 200 m.

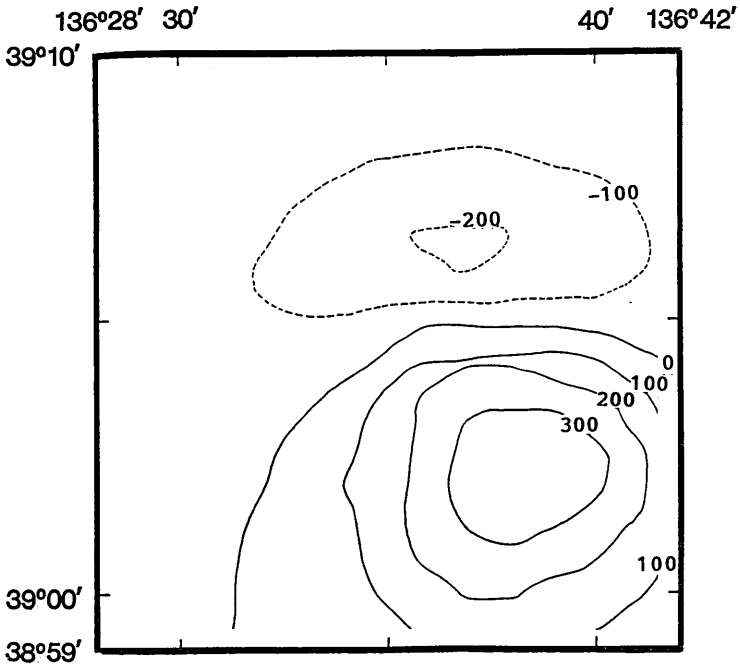

Fig. IV-11. Calculated anomaly contours of B Seamount. Contour interval is 100 nT.

As seen in Fig. IV-9, the positive anomaly is in the south of the summit and the negative one is in the north of the summit. The maximum and minimum values reach 362 nT and −249 nT respectively. It should be noted that the positive peak is located above the southeastern base of the volcano and the negative one is too far to the northwest from the summit to be interpreted as an anomaly by only the body of B Seamount above the ocean floor.

3.3. Meiyo Seamount

1) Bathymetry:

The contoured bathymetry of Meiyo Seamount is shown in Fig. IV-12.

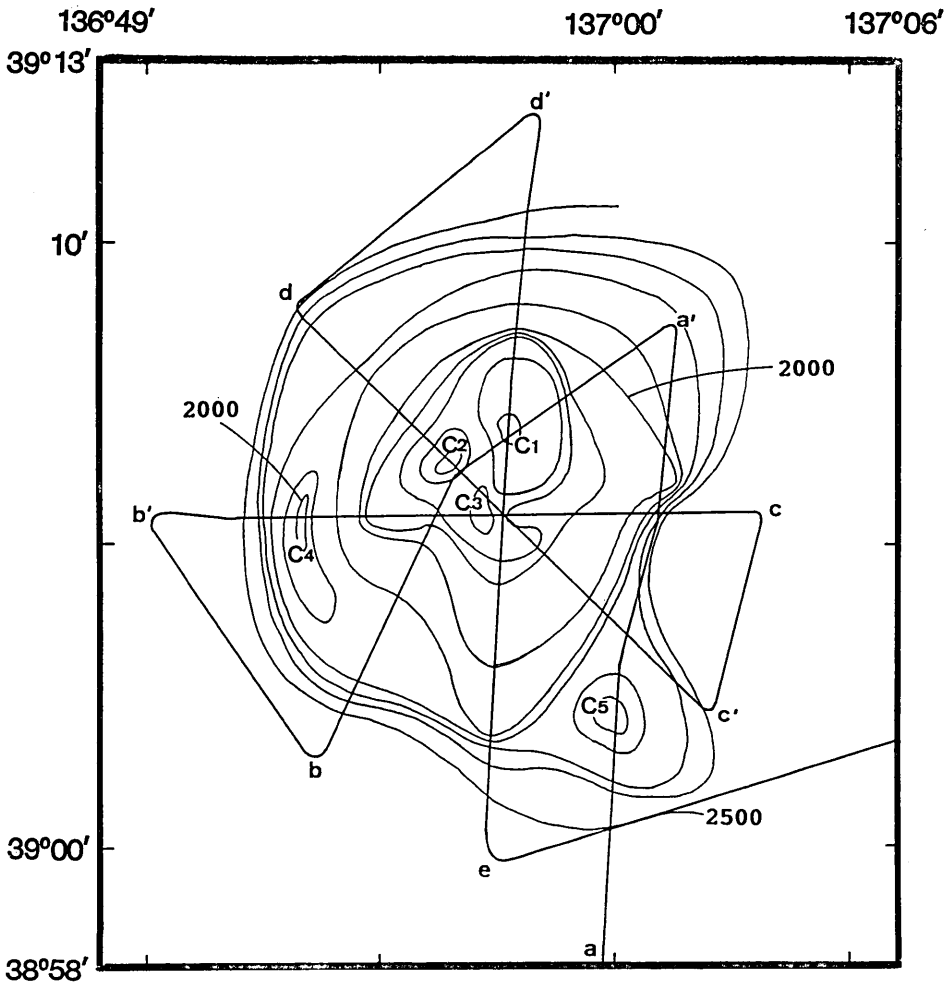

Fig. IV-12. Bathymetric contours of Meiyo Seamount. Lines a to e are ship tracks. C1 to C5 denote the bathymetric peaks. Contour interval is 100 m.

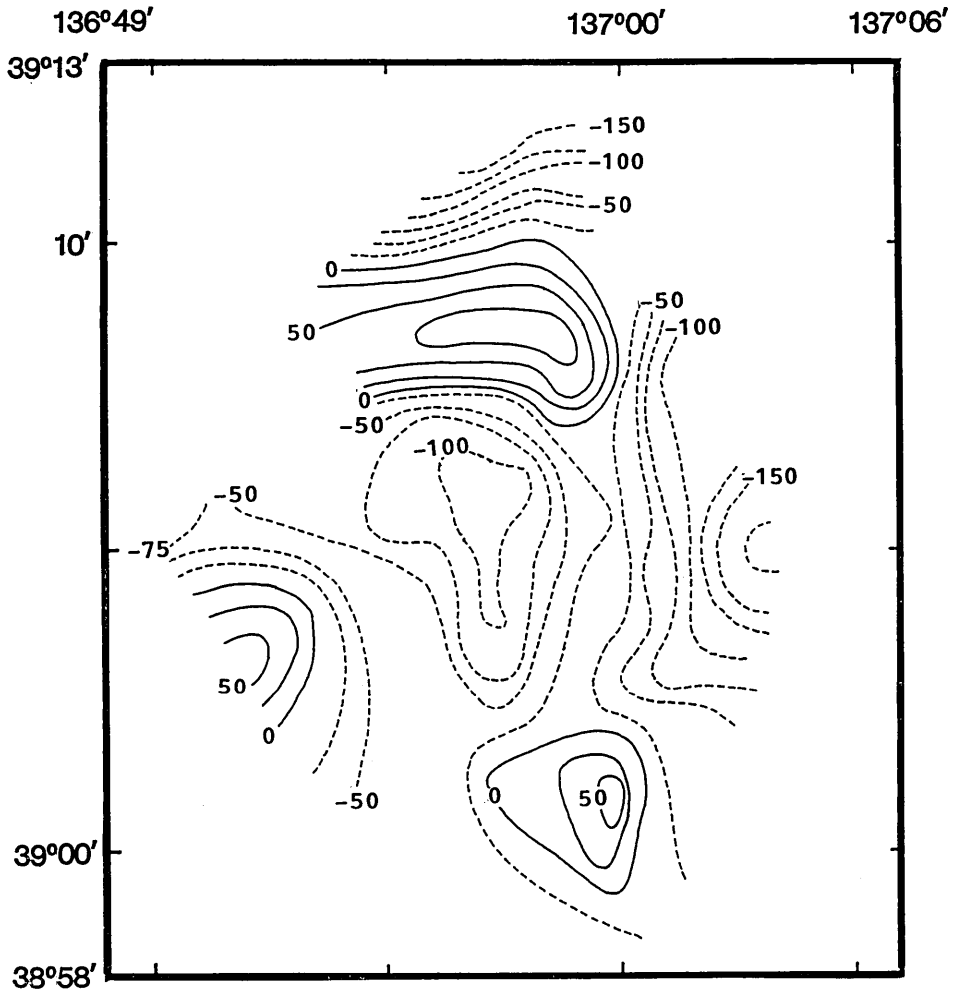

Fig. IV-13. Total intensity anomaly contours of Meiyo Seamount. Contour interval is 25 nT.

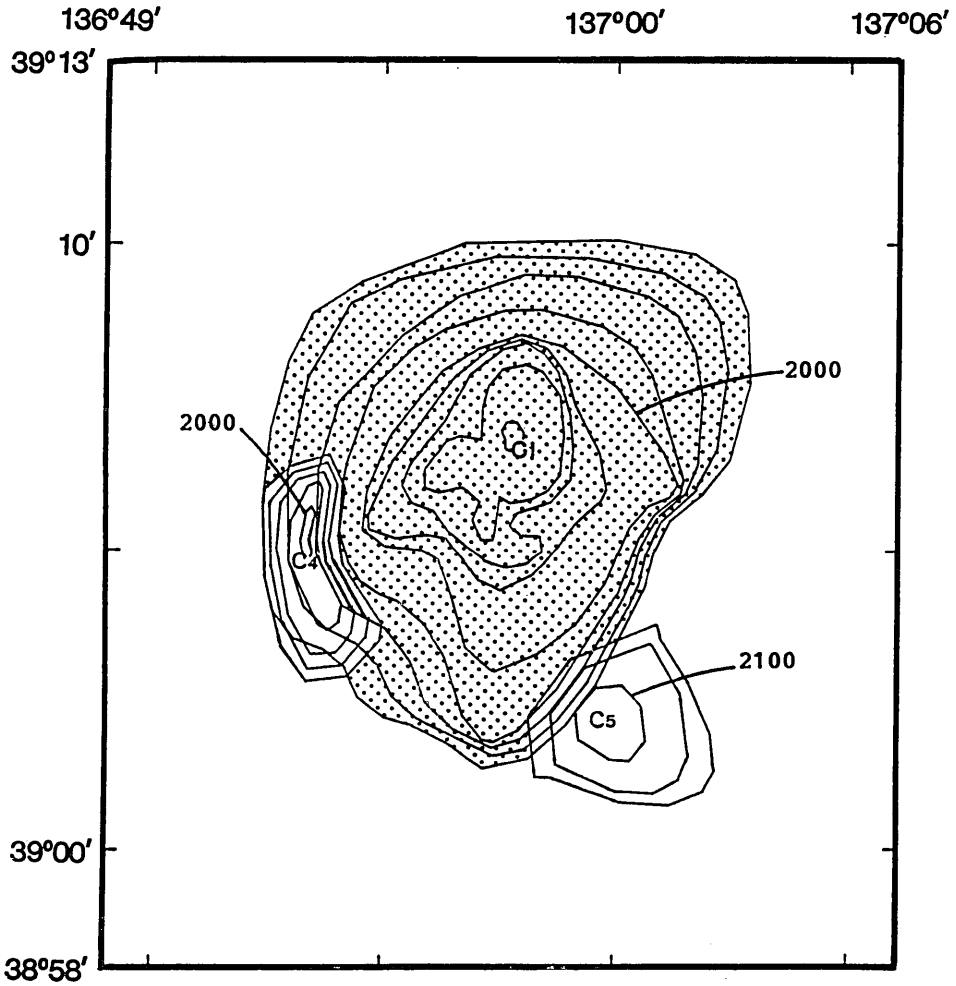

Fig. VI-14. Bathymetric model of Meiyo Seamount. The white sections are normally magnetized. The dotted section is reversely magnetized. Contour interval is 100 m.

The seamount rises about 950 m over the basin floor and reaches 1550 m from the surface. Our bathymetric data show a platform at a depth of about 1800 m. Three peaks 100 to 200 m in height sit on this platform. Two small hills are located in the direction of 160° and 245° from the summit C1 and rise about 200 m in height.

2) Magnetic Anomalies:

The anomalies over Meiyo Seamount have two minima and three maxima (Fig. IV-13). A negative peak (−114 nT) is found over the summit C2, and three positive peaks (83, 60, 58 nT) are located to the north, the south, and the southwest of the summit of the seamount.

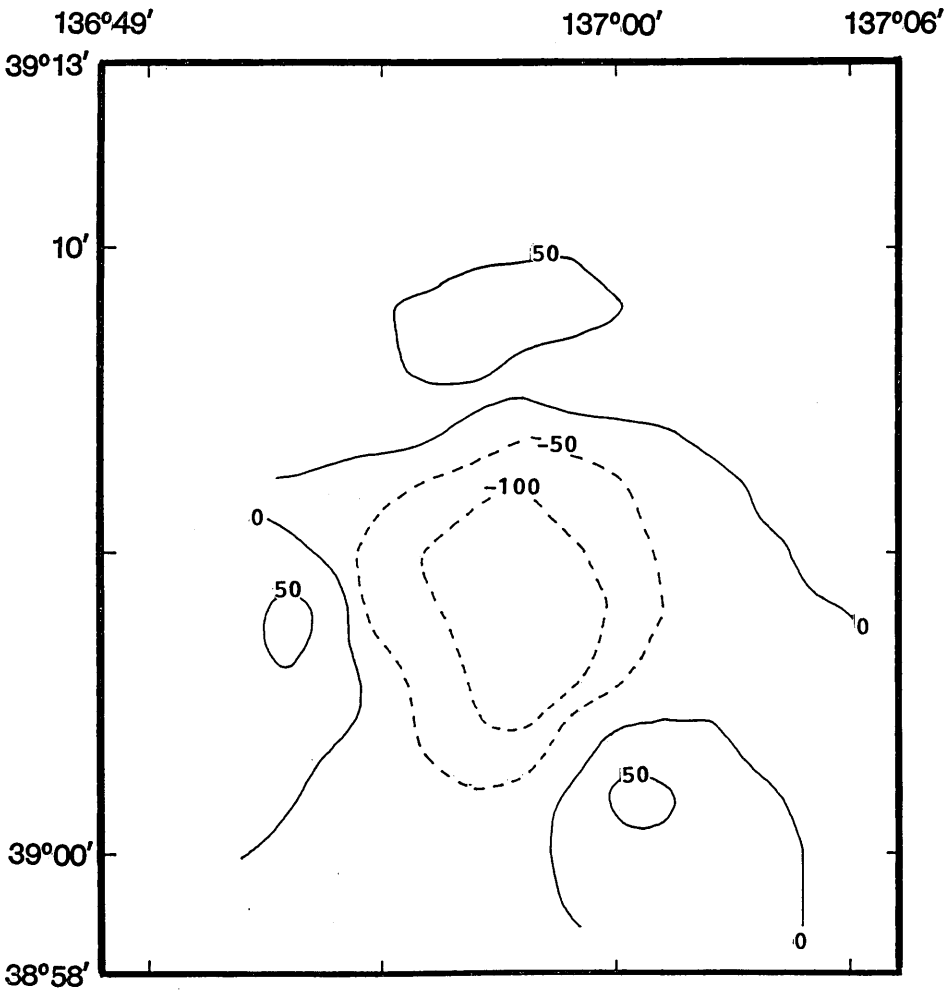

Fig. IV-15. Calculated anomaly contours of Meiyo Seamount. Contour interval is 50 nT.

3.4. Meiyo Daisan Seamount

1) Bathymetry:

Fig. IV-16 presents the bathymetry of Meiyo Daisan Seamount. The shallowest depth is 1101 m, and rises 1499 m from the ocean bottom. The seamount has a prominent topographic feature of the elongation in a north-south direction. The steepest flanks, 15°-20°, are around the summit in the northern part of the volcano. The base of the seamount appears to be buried by sediments deposited after its formation. Two small cones 200 to 300 m in height are located in the southern part of the volcano.

2) Magnetic Anomalies:

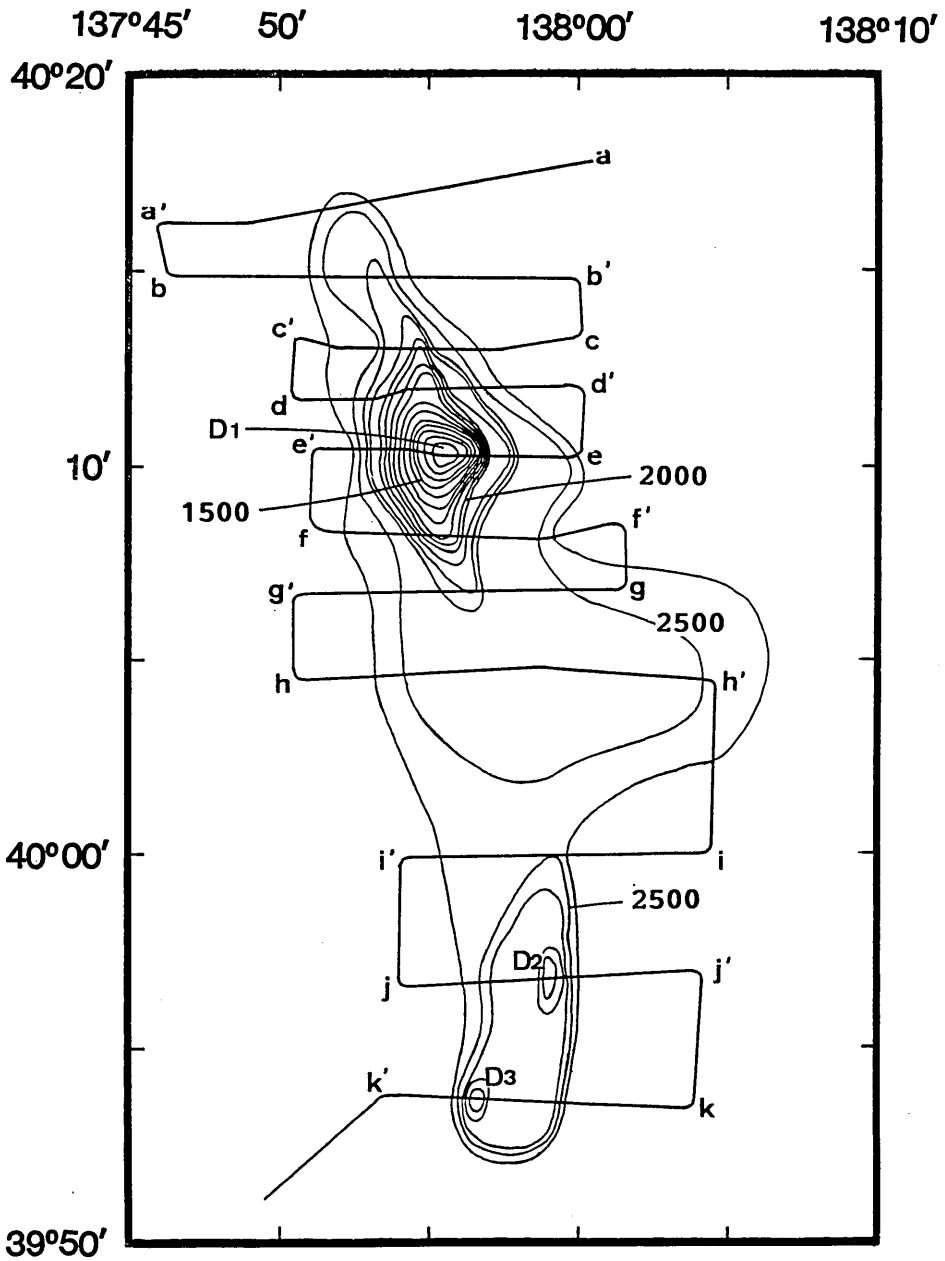

Fig. IV-16. Bathymetric contours of Meiyo Daisan Seamount. Lines a to k′ are ship tracks. D1, D2 and D3 denote three peaks of this seamount. Contour interval is 100 m.

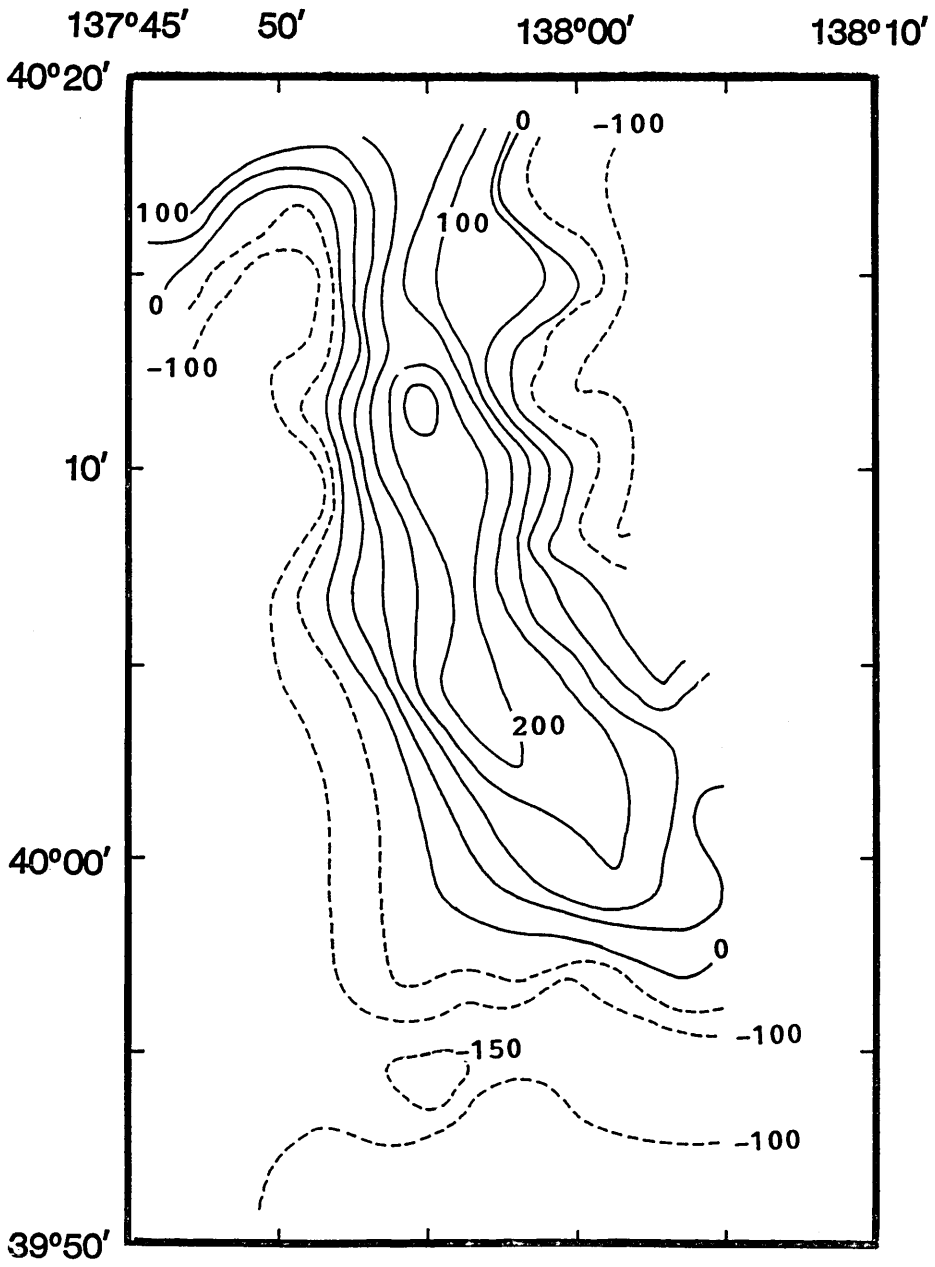

Fig. IV-17. Total intensity anomaly contours of Meiyo Daisan Seamount. Contour interval is 50 nT.

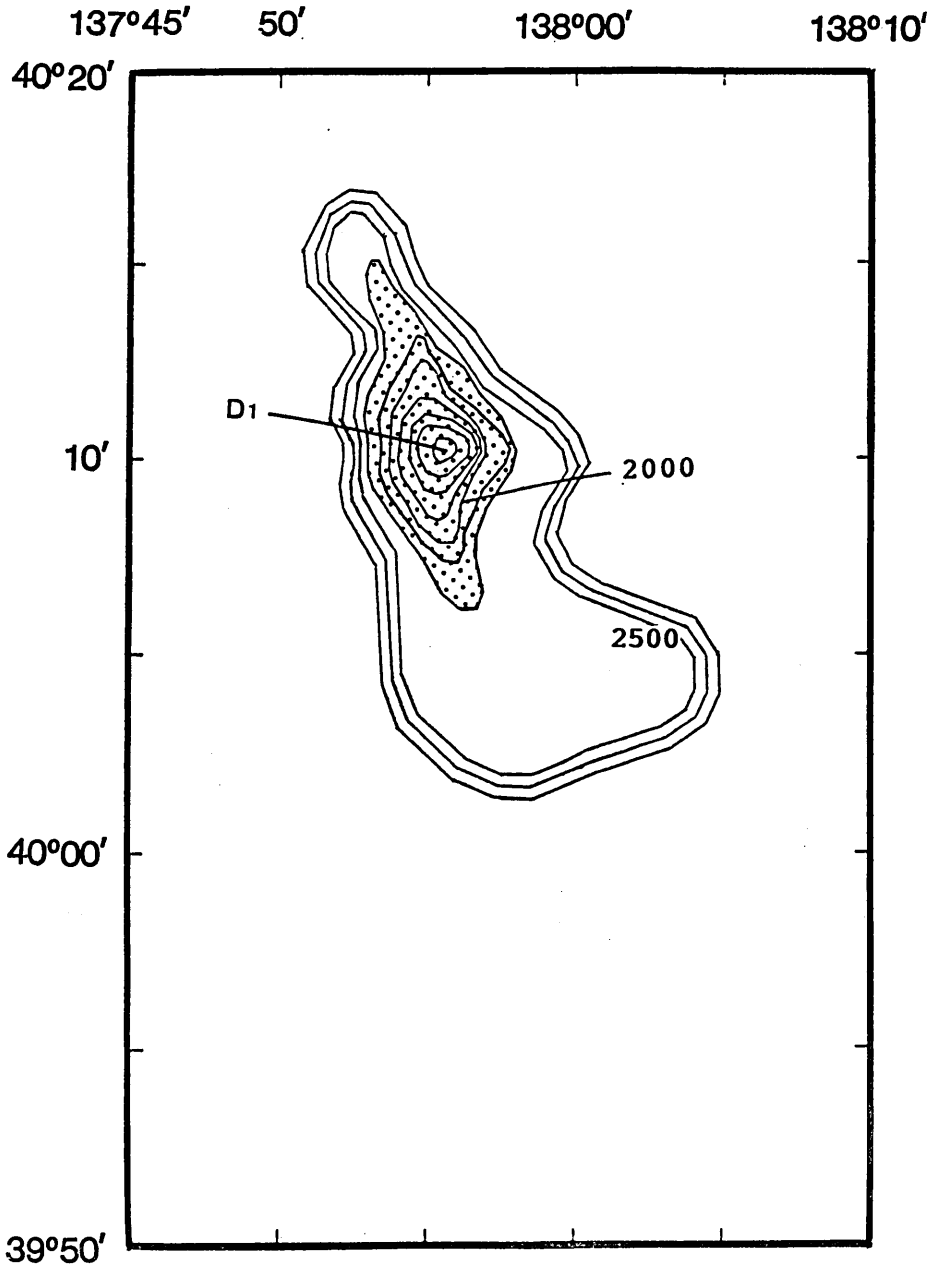

Fig. IV-18. Bathymetric model of Meiyo Daisan Seamount. The white section is normally magnetized. The dotted section is reversely magnetized. Contour interval is 200 m.

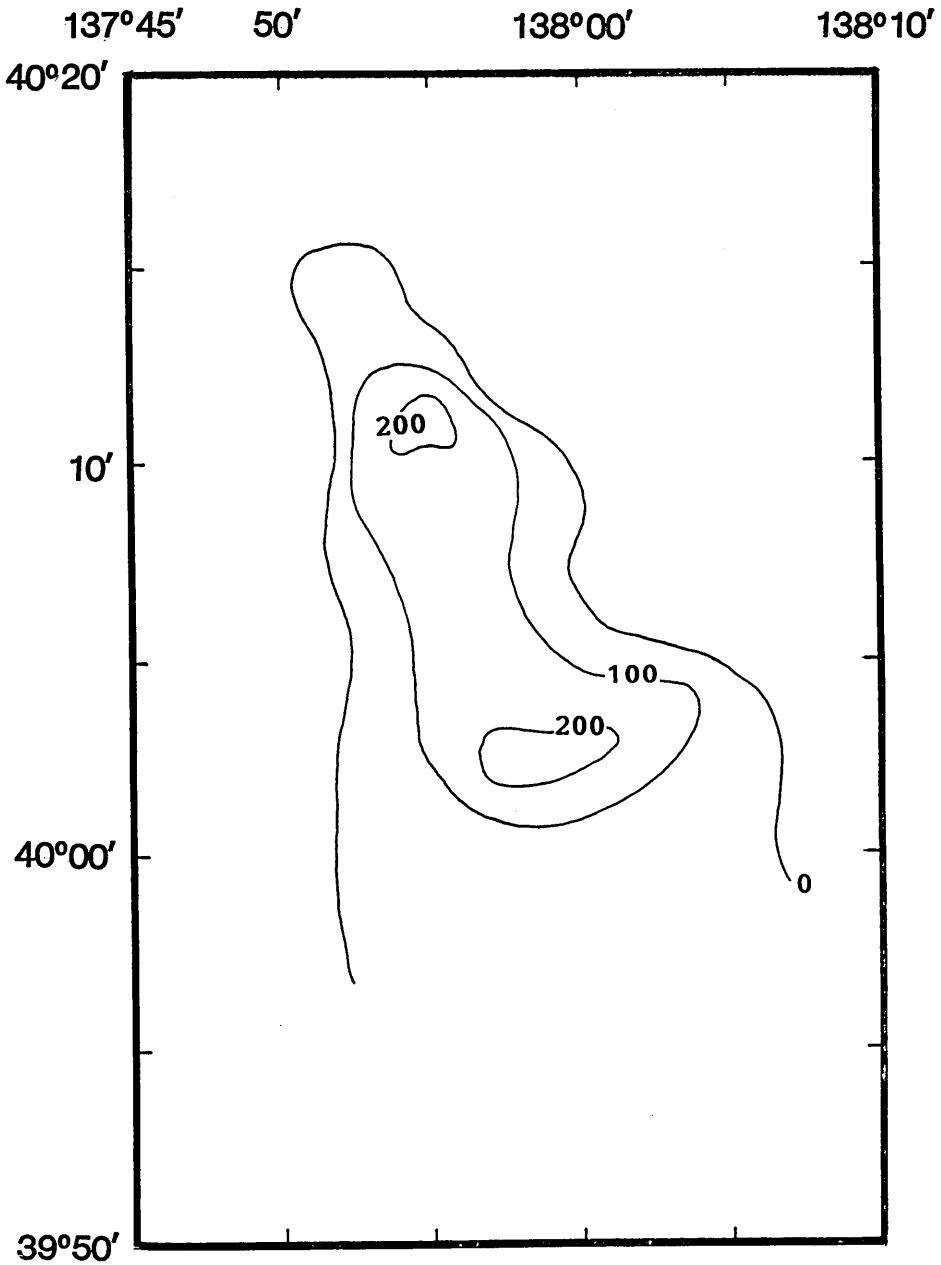

Fig. IV-19. Calculated anomaly contours of Meiyo Daisan Seamount. Contour interval is 100 nT.

As seen in Fig. IV-17, the anomalies have the overall character of a normal dipole in the northern hemisphere. The positive anomalies are present above the crests (D1 to D2 in Fig. IV-16) of the seamount. The negative anomalies are located in both the east and west sides of the positive ones. It should be noted that the peak of positive anomaly is found just north of the summit D1, with the maximum value of 263 nT. The negative peak (−155 nT) is located to the northwest of summit D3.

4. Magnetic Models

The average intensity and direction of the magnetization vector of a seamount can be computed if its shape and associated magnetic anomaly are known (*e.g.*, VACQUIER, 1962; TALWANI, 1965). The method of Talwani approximates the seamount body with a collection of horizontal polygonal laminas which are piled up in accordance with the bathymetric contours of the body. The surface integrals are performed over every lamina. The numerical integration is then carried out with respect to the z axis (TALWANI, 1965). We used this method to calculate the average magnetization vectors of the seamounts investigated in this paper.

To obtain the best models of the seamounts, the analysis was performed according to the following process:

(1) The bathymetric model for each seamount was built using the depth contours in Figs. IV-4, 8, 12, and 16. Its top and bottom were taken from the shallowest depth contour and the average basin floor depth around the seamount.

(2) The sea surface magnetic anomaly, first, was analyzed to obtain a magnetization vector using an inversion method on the assumption of uniform magnetization for the entire seamount.

(3) The magnetic anomaly from the model deduced by the above analysis was compared with the observed values. In this step we picked up discrepancies between the calculated and observed anomalies in both locations and amplitudes of positive and negative peaks.

(4) Taking the results of the step (3) into consideration, the magnetic model was modified. The major modification was that a seamount was divided into some sections with different magnetization vectors. Furthermore, we moved the bottom of a seamount farther below the basin floor and/or ignored the uppermost layers for some seamounts as the non-magnetic bodies.

In Figs. IV-6, 10, 14, and 18 we show the optimum bathymetric models for the four seamounts determined by the method described above. For B Seamount, the top of the best model is at a depth of 1900 m and the bottom is at 3500 m, i.e. 1000 m deeper than the basin floor (Fig.

IV-10). The lower part of B Seamount below the basin floor is assumed to have the same slope as the upper part. The models of the other three seamounts, the Yamato, Meiyo, and Meiyo Daisan Seamounts, require more complex modifications. The Yamato Seamount, for example, is divided into three blocks, which correspond to the peaks A2, A3, and A4, respectively (Fig. IV-6). The peak A1 was included in the block around A2. Similarly, Meiyo Seamount is modeled to have three sections, reflecting the peaks (C1, C2, C3, C4, and C5), as shown in Fig. IV-14. The three peaks, the C1, C2, and C3 in the center region of the seamount, are included in one block, C1. In Fig. IV-18, the Meiyo Daisan Seamount was split into two blocks, the upper and lower blocks of the seamount. The lower block is extended to a depth of 2700 m beneath the surrounding ocean floor (an average depth of 2600 m). In this study the southern portion of the seamount, including the peaks D2 and D3, is ignored, because the anomalies in the southern region are very poorly correlated to the bathymetry compared to those in the northern region.

We obtained the best correlation between the calculated and observed anomalies when the following magnetization parameters were adopted to the above bathymetric models:

(1) The Yamato Seamount has two normally magnetized sections (the blocks A2 and A3) and a reversely magnetized section (the block A4). The optimum declination of the blocks A2 and A3 are 0°, and the optimum inclinations are 40° and 60°, respectively. The optimum magnetization for the block A4 has a declination of 180° and an inclination of −50°. The intensities resulted in 3.0 A/m for the block A2, 6.0 A/m for the block A3, and 5.0 A/m for the block A4. The magnetic anomaly computed from this model is shown in Fig. IV-7.

(2) The magnetization of B Seamount can be obtained by one block model. The analysis gives a declination of 340°, an inclination of 40°, and an intensity of 4.5 A/m. As seen in Fig. IV-11, the positive peak of the calculated anomalies lies at almost the same location as that of the observed peak. However, the calculated negative peak is located far east of the observed negative one.

(3) Meiyo Seamount was modeled on two small normally polarized blocks on the flanks of a reversely polarized body. The block C1 has a reversed magnetization with an intensity of 2.5 A/m, a declination of 180°, and an inclination of −40°. For blocks C4 and C5, the intensities of magnetization are 6.0 and 5.5 A/m, the declinations are 0° and 10°, and the inclinations are 50° and 40°, respectively. As can be seen in Fig. IV-15, the magnetic anomaly obtained from the model agrees well with the observed anomaly.

(4) Magnetic anomalies of Meiyo Daisan Seamount are calculated by

assuming a reversely polarized summit resting on a normally porlarized base. The intensities of magnetization are 2.5 and 6.0 A/m for the upper and lower blocks of the model, respectively. The solution of the model shows that the direction of magnetization for the upper has a declination of 170° and an inclination of −30°, and that for the lower a declination of 0° and an inclination of 60°. The calculated anomaly from this model is presented in Fig. IV-19. Its correlation to the observed anomaly is the best of all experiments in this study.

Table IV-1 summerizes the results of modeling the magnetic anomaly for four seamounts. The results have two clear features. The first feature is the presence of mixed polarity in a body for three seamounts. The second one is that the declinations of all the seamounts are nearly 0° or 180°.

Table IV-1. Magnetization parameters for four seamounts.

Seamount	Peak	Polarity	Dec.('E)	Inc.('Down)	Int.(A/m)
Yamato	A1, A2	N	0	40	3.0
	A3	N	0	60	6.0
	A4	R	180	-50	5.0
B		N	340	40	4.5
Meiyo	C1, C2, C3	R	180	-40	2.5
	C4	N	0	50	6.0
	C5	N	10	40	5.5
Meiyo-Daisan	U	R	170	-30	2.5
	D	N	0	60	6.0

5. Discussion

The nonuniform magnetization models present a satisfactory explanation for the short-wavelength features of the observed magnetic anomalies, as shown in Figs. IV-5, 7, 13, and 15. For example, the negative peak over summit A4 (Yamato Seamount) and the two positive peaks over summits C4 and C5 (Meiyo Seamount) calculated with the nonuniform models are in good agreement with the observed anomalies. These peaks cannot be produced by uniform models.

Modeling for Meiyo Daisan Seamount also requires nonuniform magnetization to explain the positive peak to the north of summit D1. This seamount has two significant features. The first is that the positive

anomalies extend along the crest (D1 to D2) of the ridge. The second is that the positive peak is located to the north of summit D1. Each feature can be inferred from the normal and reversed magnetization, respectively. It is impossible to explain both two features only by a uniform model. The best model is presented when the summit of the seamount is assumed to have reversed polarity, opposite in direction to the remainder of the body.

The magnetization parameters derived from each of these models give paleomagnetic poles for four seamounts. The mean pole position is 77.2°N, 338.4°E. The 95% cone of confidence around this position is 11.9°. We calculated the expected field directions at a particular point of the Yamato Seamount Chain (39.2°N, 136.8°E) by using the apparent polar wander curve of Eurasia (IRVING, 1977) and obtained rotation angles of the area containing the Yamato Seamount Chain by subtracting the expected declination from the observed one. If the ages of the seamounts in the chain range from about 6 to 14 Ma (KANEOKA, 1986), the deviation of the observed declination at the particular position mentioned above is about 11°, counterclockwise from the expected declination. It seems likely that this apparent deviation does not represent a crustal rotation considering that the accuracy of the declination of magnetization is estimated to be about 10°.

6. Conclusions

The study of the magnetic anomalies for the four seamounts in the Yamato Basin suggests the following conclusions:

(1) Three of the four seamounts, the Yamato, Meiyo, and Meiyo Daisan Seamounts, show the presence of mixed polarity of magnetization. It suggests that the volcanism along the Yamato Seamount Chain continued over several polarity reversals.

(2) The mean paleomagnetic pole position for the four seamounts is 77.2°N, 338.4°E with an α_{95} of 11.9°. Because this pole is not significantly different from the pole obtained from the apparent polar wonder curve of Eurasia, the Yamato Seamount Chain has not been significanly rotated relative to the Eurasia continent since its generation.

References

GNIBIDENKO, H., 1979, The tectonics of the Japan Sea, *Marine Geol.*, **32**, 71-87.

IRVING, E., 1977, Drift of the major continental blocks since the Devonian, *Nature*, **270**, 304-309.

ISEZAKI, N., 1973, Geomagnetic anomalies and tectonics around the Japanese islands, *Oceanog. Mag.*, **24**, 107-158.

ISEZAKI, N., J. MATSUDA, H. INOKUCHI and K. YASUKAWA, 1981, Shipboard measurement of three components of geomagnetic field, *J. Geomag. Geoelectr.*, **33**, 329-333.

ISEZAKI, N., 1986, A new shipboard three-component magnetometer, *Geophysics*, **51**, 1992-1998.

KANEOKA, I., 1986, Constraints on the time of the evolution of the Japan Sea floor based on radiometric ages, *J. Geomag. Geoelectr.*, **38**, 475-485.

KIMURA, M., T. MATSUDA, H. SATO, I. KANEOKA, H. TOKUYAMA, N. ISEZAKI, S. KURAMOTO, A. OSHIDA, K. SHIMAMURA, K. TAMAKI, H. KINOSHITA and S. UYEDA, 1987, Report on DELP 1985 cruises in the Japan Sea, Part VII: Topography and geology of the Yamato Basin and its vicinity, *Bull. Earthq. Res. Inst., Univ. Tokyo*, **62**, 447-483.

LALLEMAND, S. and L. JOLIVET, 1986, Japan Sea: a pull-apart basin?, *Earth Planet. Sci. Lett.*, **76**, 375-389.

LUDWIG, W. J., S. MURAUCHI and R. E. HOUTZ, 1975, Sediments and structure of the Japan Sea, *Geol. Soc. Am. Bull.*, **86**, 651-664.

OTOFUJI, Y., A. HAYASHIDA and M. TORII, 1985a, When was the Japan Sea opened? Paleomagnetic evidence from Southwest Japan, in *Formation of Active Ocean Margins*, edited by N. Nasu, S. Uyeda, I. Kushiro, K. Kobayashi and H. Kagami, 551-566, Terrapub, Tokyo.

OTOFUJI, Y., T. MATSUDA and S. NOHDA, 1985b, Opening mode of the Japan Sea inferred from paleomagnetism of the Japan Arc, *Nature*, **317**, 603-604.

TALWANI, M., 1965, Computation with the help of a digital computer of magnetic anomalies caused by bodies of arbitrary shape, *Geophysics*, **30**, 797-817.

TAMAKI, K., 1985, Two modes of back-arc spreading, *Geology*, **13**, 475-478.

VACQUIER, V., 1962, A machine method for computing the magnetization of uniformly magnetized body from its shape and a magnetic survey, *Proc. Benedum Earth Magnetism Symp. Pittsburgh*, 123-137.

DELP 1985 年度日本海研究航海報告

IV. 大和海盆における海山の磁気異常

神戸大学理学部 佐柳敬造[1)]
伊勢崎修弘
北原康夫[2)]

大和海盆には大和，B，明洋，明洋第3の4海山がある．4つの海山は海盆の中軸部にあり，南西—北東の方向に海山列をつくっている．地磁気全磁力と地磁気三成分を各海山の上で観測した．全磁力異常振幅の最大値はB海山で観測された 611 nT であった．また最小値は明洋海山の 172 nT であった．観測地を説明するために，各海山に Talwani 法を適用しモデル計算をした．B海山は正帯磁に磁化し，大和，明洋，明洋第3の3海山は正帯磁と逆帯磁の部分が混在していることがわかった．B海山の偏角は 340°，伏角は 40° であった．大和海山は，2つの峰が偏角 0° 伏角 40° と偏角 0° 伏角 60° の正帯磁で残りの1つの峰が偏角 180° 伏角 −40° の逆帯磁と考えると，観測値をよく説明できた．明洋海山は中央にある峰が逆帯磁で南東部と西部の峰が正帯磁に磁化していることがわかった．逆帯磁の偏角と伏角は 180°，−40°，正帯磁の偏角と伏角は各々 0°，50° と 10°，40° であった．明洋第3海山は山体上部が逆帯磁で下部が正帯磁とすると観測値をうまく説明できた．上部の偏角は 70° 伏角は −30° で下部は偏角 0°，伏角 60° であった．正帯磁と逆帯磁の混在から大和海山列の生成期間に少なくとも1つ以上の磁場反転を含むことがわかった．また4海山の偏角が 0°（あるいは 180°）からあまりずれていないことから，大和海山列は生成後に回転しなかったものと考えられる．

現在：[1)] 東京大学海洋研究所 [2)] 小松製作所